

Experimental Study on Buckling-Restrained Knee Brace with Steel Channel Sections



Jiuk Shin

Research Specialist, Korea Institute of Construction Technology, South Korea
shinjiuk@kict.re.kr

Kihak Lee

Associate Professor, Sejong University, South Korea
kihaklee@sejong.ac.kr

Seong-Hoon Jeong

Assistant Professor, Inha University, South Korea
jeong@inha.ac.kr

Han-Seon Lee

Professor, Korea University, South Korea
hslee@korea.ac.kr

SUMMARY:

In this paper, Buckling-Restrained Knee Bracing (BRKB) systems were developed through sub-assembly tests. The steel core plate of the BRKB was restrained with two steel channel sections and is intended to retrofit existing low-story building structures for earthquake loadings. Five BRKB specimens were developed considering important variables that affected the lateral resisting capacity. Tests of the five BRKBs were carried out under cyclic loading as specified in the AISC2005 Seismic Provisions. It was observed that the ductility and energy dissipation capacity of the BRKBs were mainly affected by the size of core plate and the size of channel sections compared to the size of the end plate. Through a sub-assembly test, five specimens satisfied the compression-strength adjustment factor's requirement (≤ 1.3) in the AISC2005 Seismic Provision and four specimens exceeded requirement of the cumulative plastic ductility (≥ 130) specified in the AISC-SEAOC. The test results showed that the installation of the BRKB systems to the existing buildings can be considered as one of the effective retrofit procedures for existing low-story buildings.

Keywords: Buckling-Restrained Knee Brace; Sub-assembly test; Piloti type reinforced concrete building; Seismic Retrofit

1. INTRODUCTION

The present study investigates the use of a steel knee bracing for seismic retrofit of a low-rise multi-unit residential structure. Since steel knee bracing can be installed in proximity to the beam-column joint area, they do not restrict the parking area. In addition, ease of constructability of the knee bracing system, in contrast to the addition of shear walls, makes it possible to carry out the seismic retrofit without any inconvenience to residents as demonstrated in the previous studies (Balendra et al., 1991; Suita et al., 2006). However, bracing systems are generally vulnerable to cyclic loadings such as earthquake ground motions, due to buckling under compression. Thus a buckling-restrained brace (BRB) is considered in this study, which shows large inelasticity without buckling under compression. The detailed information of BRBs is given in elsewhere (Takeuchi et al., 2010).

Many researchers have carried out experiments and numerical analyses of BRBs for incorporation into a seismic force resisting system. Yoshino and Karino (1971) performed tests on a brace element comprised of a flat steel plate (a core plate) and reinforcing concrete panels (as a restrainer) with debonding material. The debonding material was used to avoid attachment between the core plate and the restrainer. Watanabe et al. (1988) found that the elastic buckling strength of the restrainer should be larger than the yield force of the core plate for preventing overall flexural buckling of the BRB. Studies on practical applications of BRB to buildings were conducted by Qiang (2005), and design procedures incorporating BRBs into building structures were suggested by Clark et al. (1999) and Choi and Kim (2009). Modeling of hysteretic curves by component tests of BRBs was carried out by Black et al. (2004). From the tests and analysis results, it was concluded that a BRB can be used as a practical and reliable alternative to conventional lateral load resisting systems. A new

type of BRB, a double-Tee double-tube BRB (DT-BRB), was suggested by Tsai et al (2002). Pseudo-dynamic experiments and numerical analyses of a large scale frame with BRBs were conducted by Fahnestock et al. (2004), and it was found that the connection at the ends of the BRB should have sufficient stiffness and strength for maintaining stable behavior under maximum compression and tension force. Experimental and analytical studies of a knee brace system were performed by many researchers. Aristizabal-Ochoa (1986) developed a Knee Braced Frame (KBF) as a new alternative structural system for earthquake-resistant steel buildings. Sam et al. (1995) carried out pseudo-dynamic testing of single and double story KBF models, and showed that the knee brace systems were enough to reduce the damage due to the earthquake loadings effectively and economically.

The aim of the present research is to develop a buckling restrained knee bracing (referred to as BRKB) systems composed of a steel core plate restrained by channel sections. For a typical BRB or BRKB, buckling is inhibited by a concrete or mortar filled steel tube. However, the BRKB system developed in this study uses the steel channel sections. The developed system was to increase the quality in manufacturing process, and have flexibility in the design details at both ends of the core plate. The BRKBs are installed in a 1-bay 1-story steel frame and tested under cyclic loading to verify the seismic performance.

2. DESIGN OF A BUCKLING-RESTRAINED KNEE BRACE

In this study, a total of five BRKB specimens were manufactured and tested under cyclic load. Design variables for the five test specimens were the size of the core plate (aspect ratio of the core plate), the size of the channel sections (or P_{cr}/P_y), and the size of the end plate (aspect ratio of the end plate). Details of the specimens are summarized in Table 1, where the letters C and R in the naming of the specimens denote the core plate and the channel sections, respectively. The numbers following C and R represent the width of the core plate and the web length of the channel section, respectively. Dimensions and drawing details of a typical specimen used for this study are shown in Figure 1. In Figure 1, the core plate was designed to resist the axial force transmitted to the brace, and the channel sections were used to restrain the core plate from buckling. Debonding material (rubber) was used for minimizing friction occurring between the channel sections and core plate. Guide plates were added to each specimen to prevent buckling of the end plates. Grooves at the ends of the channel section were cut in order to prevent contact between the guide plates and the channel sections.

For the design of the BRKB, the maximum of axial force of the core plate was assumed as the maximum capacity of an actuator used in this test, and 42x16mm (2.60:1) and 60x16mm (3.75:1) core plates were designed using ductility demands of the brace calculated by 1.50% and 3.0% allowable inter-story drift ratio, respectively. The sizes of the channel sections were determined based on the findings from the previous research performed by Watanabe et al. (1988) who suggested that the yield strength (P_y) of the core plate should be larger than the buckling strength (P_{cr}) of the channel section ($P_{cr}/P_y > 1.0$) to prevent buckling of the core. For the specimen with the 42x16mm core plate, two different P_{cr}/P_y of the channel sections were used; i.e. $P_{cr}/P_y = 2.53$ (100x50x5x7.5mm) and $P_{cr}/P_y = 9.41$ (150x75x6.5x10mm). For the specimen with the 60x16mm core plate, P_{cr}/P_y of the channel sections corresponded to 1.78 (100x50x5x7.5mm) and 6.59 (150x75x6.5x10mm). In this study, the dimension of the non-retrofitted parts including the end plate was determined using Eq. (1) proposed by Tsai et al. (2002) for preventing buckling of the parts. They showed that the buckling strength of the ends of the brace, computed using the following equation, should be larger than the maximum compression force.

$$P_{e_trans} = \frac{\pi^2 EI_{trans}}{(KL_u)^2} \times P_{max} \quad (1)$$

Where P_{e_trans} is the buckling strength of the end of the brace, I_{trans} is the second moment of inertia of the end of the core plate, and L_u is the length of the non-retrofitted section. In order to connect the two restrainer channel sections, 80x60mm stiffeners were welded to the channel sections at a uniform interval. The stiffeners were welded at the top and bottom of the channel sections. The number of stiffeners was determined such that the buckling of the parts between the stiffeners would

be prevented under the maximum compressive forces. In order to prevent the local buckling, it is very important that only steel-encased BRBs minimize friction forces occurring between the core plate and channel sections. Tremblay et al. (2006) discussed the role of a gap between the core plate and the steel restrainer in both directions, and Mehmet et al. (2010) used four layers of 0.05 mm-thick polyethylene film and grease in order to reduce the frictional force. In this study, instead of providing a gap, a 2mm-thick rubber sheet was placed as a debonding material between the core plate and the channel sections as depicted in Figure 1.

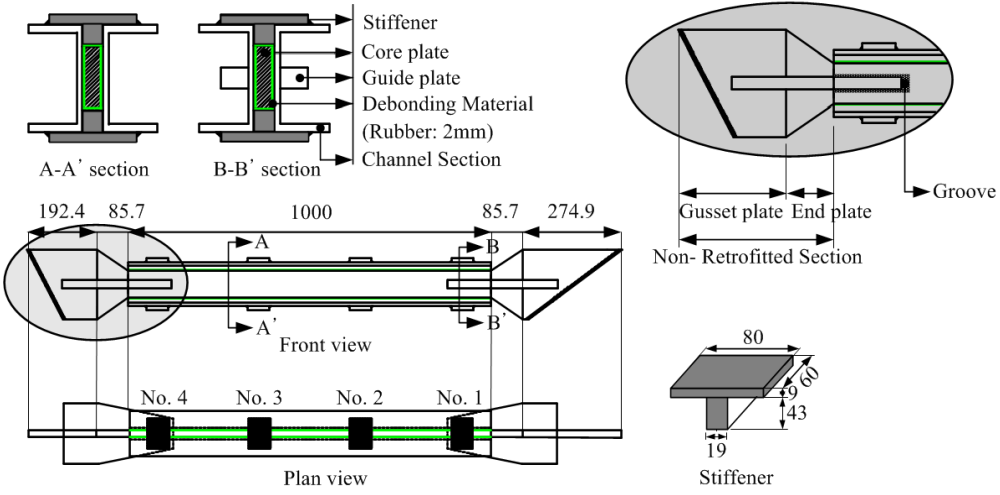


Figure 1 Details of a typical specimen

3. TEST PLAN AND SPECIMEN INSTALLATION

A schematic drawing and a photograph of the pin-connected 1-bay 1-story test frame (5.87m×2.93m) with a BRKB specimen are shown in Figure 2. Bearings were placed at the upper and lower joints of the vertical steel member to simulate desired behavior of the pin connection. With this configuration, only the BRKB resist lateral loading, and thus the loading is not transferred to the supporting frame. Cyclic loading was applied to the frame with a hydraulic actuator installed between the upper horizontal loading frame and the reference wall (Figure 2). The loading step of each specimen was determined by the specifications of the AISC 2005 (2005) as illustrated in Figure 3. The loading protocol was established up to 3.0% of the inter-story drift ratio of the steel frame. This is twice the maximum design story drift (Δ_{bm}) specified in the AISC Seismic Provisions, which is 1.5% of the story height. The first set of the loading cycles (1st and 2nd steps) was applied to the test frame within an elastic range. This is intended to reduce experimental error and allow observation of the initial behavior of the brace prior to plastic deformation. Two cycles of loading were applied for each target drift of 0.75%, 1.5%, 2.25%, and 3.0% inter-story drift ratios. After reaching 3.0% of the inter-story drift ratio, four cycles of 2.25% inter-story drift (11th-14th loading steps) were additionally applied to the test frame in order to satisfy the AISC2005 specification, which requires the cumulative inelastic strain more than 200 times of the yield strain. Afterwards, if the brace had not fractured within the above AISC 2005 loading steps (1st-14th loading steps), the ultimate resisting capacity of the brace was investigated by applying four loading steps (15th-18th loading steps). In each cycle of the latter loading steps, the test frame was pushed to the inter-story drift ratios of 3.75%, 4.50%, 5.25%, and 6.0% which are 2.5, 3.0, 3.5 and 4.0 times the design story drift (Δ_{bm}), respectively.

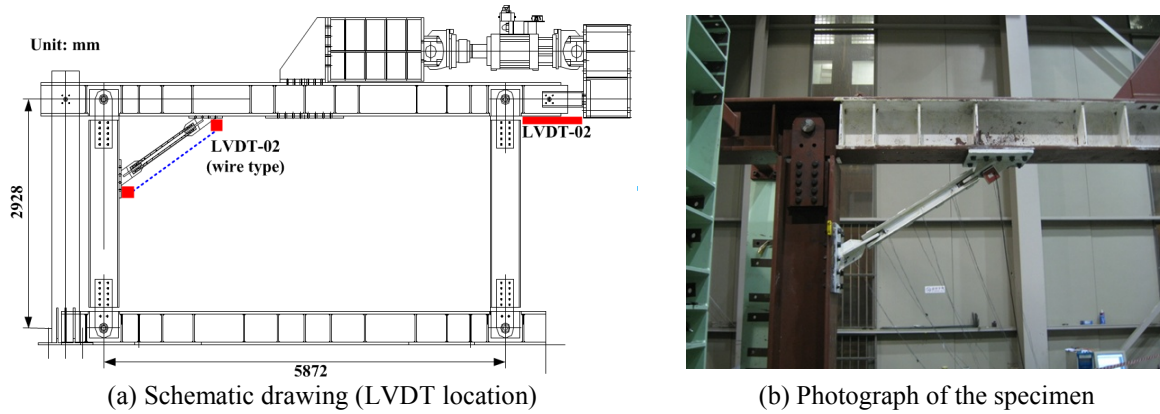


Figure 2 Schematic drawing & photograph of test setup

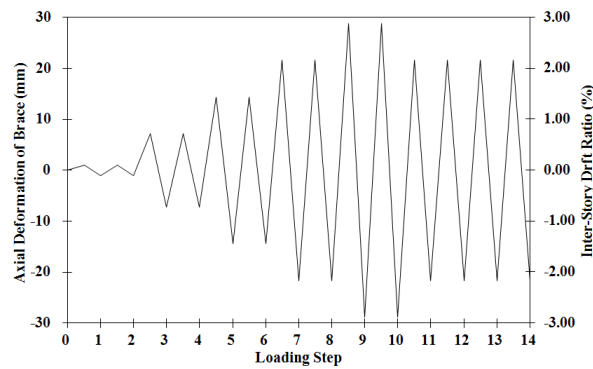


Figure 3 Loading protocol specified in the AISC Seismic Provisions

4. TEST RESULTS OF THE BRKB SPECIMENS

4.1 Hysteretic Behavior and Failure Modes

Axial force-deformation relationships obtained from the experimental results of the five BRKB specimens are presented in Figure 4. The failure modes of the C60R100 and C60R150 specimens are shown in Figure 5. The C42R100-1 exhibited no significant deformation except for cracking of the plaster at the surface and rubber detachment at the upper and lower parts of the brace up to the 6th loading step (1.5% inter-story drift ratio). At the 8th loading step (2.25% inter-story drift ratio), some cracks of the plaster at the stiffeners were observed due to in-plane buckling of the core plate. The No. 2 stiffener was detached from the brace at the 10th loading step. The detachment, which was resulted in a loss of confinement, occurred due to the strong axis buckling of the core plate. The experiment was stopped due to a fracture of the core plate at the 14th loading step (four cycles of 2.25% inter-story drift ratio as shown in Figure 3).

The C42R100-2 specimen served as a reference model among the five specimens. The only difference between C42R100-1 and C42R100-2 was the size of the end plate; 160x19mm and 120x19mm for C42R100-1 and C42R100-2, respectively. The C42R100-2 displayed a similar behavior to that of the C42R100-1 until the 10th loading step was reached. The core plate and the channel sections of the latter specimens did not show significant deformation up to the 6th loading step (1.5% inter-story drift ratio). At the 8th loading step (2.25% inter-story drift ratio), gradual in-plane buckling of the core plate was observed. After the 10th loading step (3.0% inter-story drift ratio), detachment of No. 3 stiffener was observed with an increase of the axial deformation of the specimen. Global buckling of the core plate in strong axis was observed at the 13th loading step (four cycles of 2.25% inter-story drift ratio in Figure 3). The failures of the C42R100-1 and C42R100-2 occurred due to detachment of the stiffeners leading to loss of confinement of the core plate. In terms of the axial force capacities, there was less than 2% difference at each step between the C42R100-1

and C42R100-2 (Figure 4 (a) and (b)). Through this comparison, it was observed that the size of the end plate did not significantly affect the axial force of the brace.

The C42R150-R specimen was designed with an increase of the channel section size; 150x75x6.5x10mm compared to 100x50x5x7.5mm of the aforementioned C42R100-1 and C42R100-2 specimens. As a result, the ratios P_{cr}/P_y for the C42R100 and C42R150-R specimens are 2.53 and 9.41, respectively. The confinement effect of the channel sections was investigated using the two specimens. In all specimens except the C42R150-R, uniform core plate sections of 42x16 mm were used along the whole longitudinal length as a main force resisting element. On the other hand, for the C42R150-R specimen, the core plate at the ends was enlarged to 75.2x16mm in order to enhance the buckling strength. The C42R150-R specimen showed minimal deformation up to the 6th loading step (1.5% inter-story drift ratio). Out-of-plane buckling at the ends of the core plate was observed after the 6th loading step. The brace was fractured under the tension force at the 10th loading step (3.0% inter-story drift ratio). Unexpectedly, despite the larger size of channel sections and the core plate, the end of the C42R150-R buckled at an earlier loading step. In this specimen the guide plate was designed longer than other specimens; as a result, the groove length of the C42R150-R had to be designed longer than those of other specimens. Due to the longer groove length, larger stresses were concentrated at the groove and the specimen failed in an earlier loading stage.

The width of the core plate was increased in the C60R100 specimen compared to the three C42R specimens. As shown in the hysteresis curve of Figure 6(d), it displayed the most stable hysteretic behavior among all five test specimens as well as the best energy dissipation capacity. It also showed no significant deformation up to the 8th loading step (2.25% inter-story drift ratio). Cracks of the plaster at the surface of the channel sections occurred at the 10th loading step (3.0% inter-story drift ratio). However, only a few cracks were observed visually at the stiffeners, channel sections, etc. up to the 14th loading step (four cycles of a 2.25% inter-story drift ratio in Figure 3). After applying additional loading steps, in-plane buckling of the core plate was observed at an inter-story drift ratio of 3.75%. Significant deformation was observed at No. 2 and No. 3 stiffeners at the 16th loading step (4.5% inter-story drift ratio), as shown in Figure 5. Local buckling of the channel sections occurred with deformation of the stiffeners. Although in-plane and out-of-plane buckling of the core plate occurred at the additional loading steps, the core plate still remained and was well restrained by the channel sections and stiffeners. Finally, fracture of the core plate occurred at the 17th loading step (5.25% inter-story drift ratio), with axial displacement of 45.12mm under the tension force.

The specimen C60R150 with a core plate of 60x16mm (aspect ratio=8.42:1) and two channel sections of 150x75x6.5x10mm ($P_{cr}/P_y = 6.59$) was designed to have larger channel sections than the specimen C60R100 in order to investigate the confinement effect of the channel sections. As shown in Figure 6(e), the hysteresis curve is stable and excellent energy dissipation capacity similar to that of the specimen C60R100 was obtained. The hysteresis loops of the C60R150 showed asymmetric shapes between the tension and compression. The asymmetric hysteresis loops were attributed to the slips occurring during the test. The specimen underwent no significant deformation until the 10th loading step (3.0% inter-story drift ratio); only cracking of the plaster on the surface of the channel sections was observed. Cracks of the plaster of the stiffeners and deformation of the core plate started at the 12th loading step (four cycles of 2.25% inter-story drift in Figure 3). Before the additional loading steps (15th-18th loading steps in Figure 3) were applied, there was no significant deformation in the channel sections. As the C60R150 specimen was composed of larger channel sections than those of the specimen C60R100, it was expected that the performance of the former would be better than that of C60R100. However, this specimen failed to exhibit full capacity due to local buckling at the end of the channel sections. During the test the rubber sheet at the end of the core plate was detached followed by the damage at the end of the core plate. When the additional loading steps were applied, an end of the core plate buckled and then the specimen fractured at the 16th loading step (5.25% inter-story drift ratio) as shown Figure 5(b).

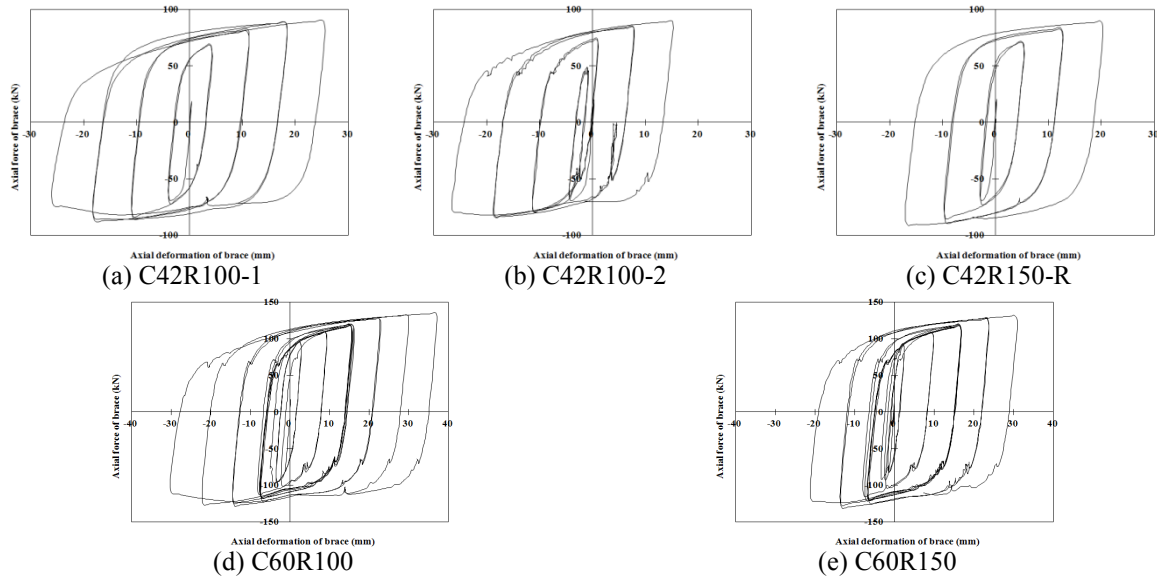


Figure 4 Load-displacement hysteresis curves of the BRKBs



Figure 5 Failure modes of C60R100 and C60R150 specimens

4.2 Compression-strength adjustment factor (β)

The AISC Seismic Provisions (2005) specifies the compression-strength adjustment factor (β) for BRBs. The β factor is the ratio of the maximum compression strength to the maximum tension strength of the test specimen, measured from qualification tests for a range of deformations corresponding to 2.0 times the design story drift. The compression strength of a BRB is generally larger than the tension strength due to the confinement of the restrainers. For inverted-V-type bracing, when the β factor is too large, the beam intersected by the BRB can be fractured due to unbalanced force in the vertical direction. The Seismic Provisions specify that the β factor should not exceed 1.3. Based on the experimental results, the β factor of the BRKB specimens was calculated and the results are presented in Figure 6. The β factors for C42 and C60 specimens are depicted in Figure 6(a) and 6(b), respectively. Overall, the specimens satisfied the limit of the β factor specified in the Seismic Provisions. The β factor gradually decreased when the axial deformation of the brace increased due to local buckling at the channel sections. Figure 6(a) shows that the β factor of the specimen C42R150-R was larger than those of the specimens C42R100-1 and C42R100-2. Figure 6(b) shows that C60R150 has a larger β factor than C60R100 during the specified loading steps. However, after the additional loading steps, the β factor of the specimen C60R150 steeply declined. This was because the specimen could not resist the compression force from the additional loading steps due to buckling at the end of the core plate.

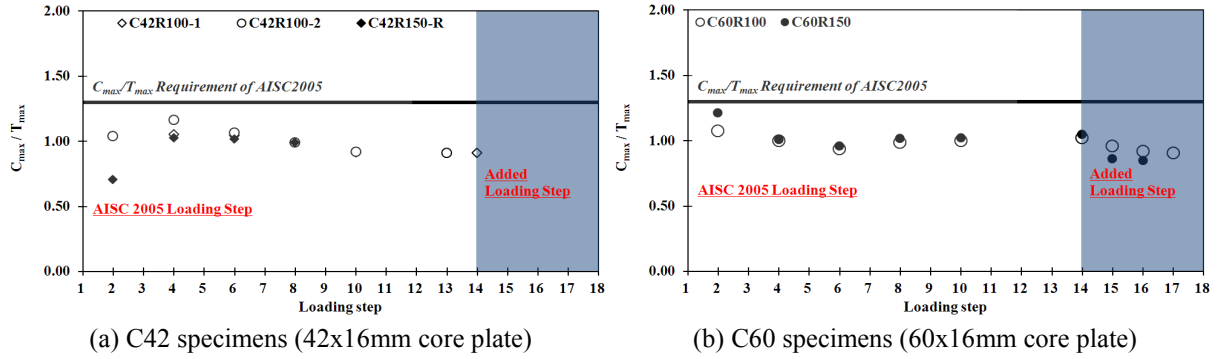


Figure 6 Compression-strength adjustment factor for the C42 and C60 specimens

4.3 Comparison of Plastic Ductility (μ) of the Specimens

The cumulative plastic ductility (CPD) of each specimen was calculated by summation of the ductility of each cycle. The cumulative plastic ductility was obtained by a ratio of the difference between the maximum tension deformation (u_{pi}^{max}) and the maximum compression deformation (u_{pi}^{min}) over the yield deformation (u_y) with respect to each loading cycle as defined in the AISC Seismic Provisions (2005) and in the AISC-SEAOC (Structural Engineers Association of California) Recommended Provisions for Buckling-Restrained Braced Frames (2005). The Seismic Provisions stipulate that the brace test specimen must achieve a cumulative inelastic axial deformation of at least 200 times the yield deformation (more than the cumulative plastic ductility of 200). The Recommended Provisions for Buckling-Restrained Braced Frames require that the cumulative plastic ductility of the BRB be at least 140 times the yield deformation.

In this study, it was observed that four specimens (C42R100-1, C42R100-2, C60R100 & C60R150) exceeded the cumulative plastic ductility of 140 specified in the AISC-SEAOC (Figure 7(b)) while all specimens did not satisfy the CPD requirement of AISC Seismic Provisions (Figure 7(a)). When the additional loading steps were used, C60R100 and C60R150 specimens exceeded the CPD requirement of the AISC. Unlike a component test, the sub-assembly test may have a difficulty involved with the connection between brace and test frame. In this study, unexpected slips occurred in the connections during the sub-assembly test which significantly affected the test results. As shown in Figure 4, the axial deformation of some specimens at each loading step was directed toward compression or tension side due to the slips, which resulted in the reduced CPD within the specified loading steps. It should be noted that the cumulative plastic ductility in the Seismic Provisions is required only for the BRB component test, not for the sub-assembly test. Therefore the test results obtained in this study do not imply that the seismic performance of the specimens is not satisfactory.

The cumulative plastic ductility computed for each specimen is shown in Figure 7. In Figure 7(a), C42R150-R has the largest ductility until the 8th loading step (2.25% inter-story drift ratio), but the ductility of C42R150-R declined starting from the 10th loading step (3.0% inter-story drift ratio). This is due to the fracture at the end of the core plate resulting from concentrated stresses around the groove. Both C42R100-1 and C42R100-2 specimens were satisfied based on the requirement of cumulative plastic ductility specified in the AISC-SEAOC. The cumulative plastic ductility of C60 specimens is shown in Figure 7(b). While both specimens failed to satisfy the cumulative plastic ductility of 200 specified in the Seismic Provisions within the loading step, they met the CPD requirement of AISC-SEAOC (more than 140). The two specimens showed a similar trend for cumulative plastic ductility. The cumulative plastic ductility of the C60R150 specimen was larger than that of the C60R100 due mainly to the improvement of the confinement with increase of the size of the channel sections.

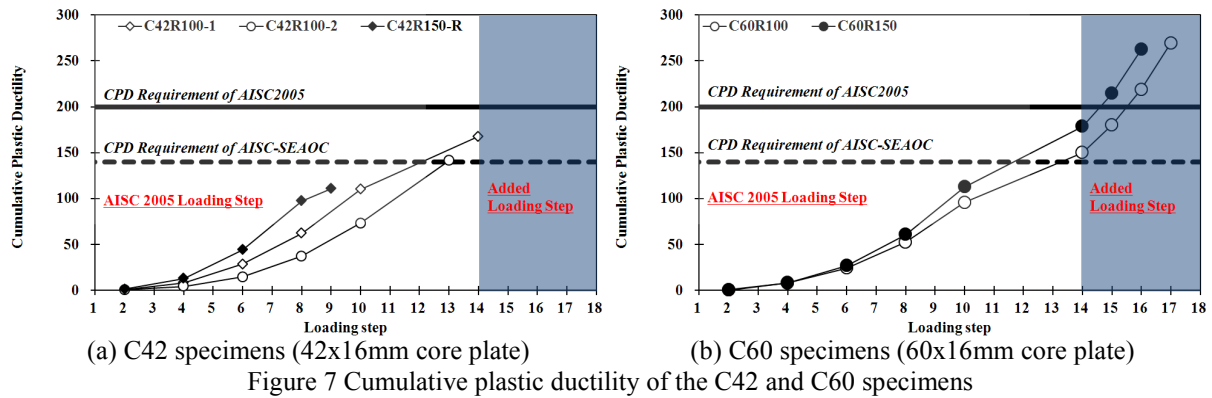


Figure 7 Cumulative plastic ductility of the C42 and C60 specimens

4.4 Comparison of Energy Dissipation Capacity

Energy dissipation capacity was computed by the area surrounded by the load-displacement hysteretic curve of each specimen and then the cumulative hysteretic energy was computed by summing the energy dissipation capacity of the specimen with respect to each cycle as described in Horie et al. (1993) and Black et al. (2004). Figure 8 shows the cumulative hysteretic energy of each test specimen. Among the C42 specimens, the C42R100-1 showed the most stable hysteretic curve and the largest energy dissipation. The specimen C42R150-R showed similar energy dissipation capacity to C42R100-2 specimen before fracture of the core plate at the 8th loading step (2.25% inter-story drift ratio), the energy dissipation of the specimen C42R150-R abruptly decreased. The specimen C42R100-1 displayed similar energy dissipation to C42R100-2 as can be observed in Figure 8(a). The specimens C60R100 and C60R150 dissipated almost the same energy within the AISC loading steps, as shown in Figure 8(b). After the additional loading steps, the energy dissipation capacity of the specimen C60R150 was less than that of C60R100 due to the occurrence of local buckling of the core plate as a result of the reduced confinement effect of smaller channel sections (Figure 8(b)). The C60 specimens (C60R100 & C60R150) dissipated roughly twice greater energy than C42 specimens (C42R100-1, C42R100-2, and C42R150-R).

From the test results, it was concluded that the BRKB made of a core steel plate confined with channel sections satisfied the β factor requirement of the AISC Seismic Provisions and the CPD of the AISC-SEAOC. The confinement of the channel sections was sufficient to prevent buckling at the core plate within the loading steps specified in the Seismic Provisions. Cumulative hysteresis energy of the C60R100 (76750kN-mm) is larger than about 20% that of the C60R150 (63400kN-mm) at the last loading step of the each test model. The C60R100 specimen showed the best load resisting capacity among the five specimens. This specimen had the largest cumulative energy dissipation capacity and satisfied the requirements for the β factor and cumulative plastic ductility specified in the provisions during the loading steps used in the experiment (AISC loading steps & additional loading steps).

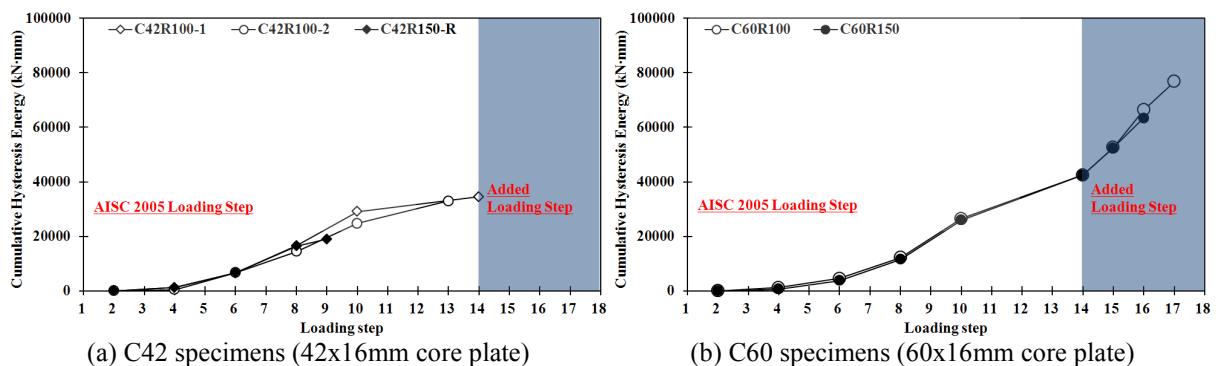


Figure 8 Cumulative hysteretic energy of the C42 and C60 specimens

6. CONCLUSIONS

Experimental study was carried out to investigate a buckling-restrained knee brace (BRKB) for seismic retrofit. The findings of this study are summarized as follows.

In the sub-assembly tests of the developed BRKB specimens, ductile force-displacement relationships were observed. All BRKB specimens satisfied the requirement for the compression-strength adjustment factor specified in the AISC Seismic Provisions. The cumulative plastic ductility (CPD) of the test specimens except the C42R150-R specimen exceeded the requirement (>140) specified in the AISC-SEAOC provisions; while no specimen satisfied the requirement (>200) specified in the AISC Seismic Provisions due to the unexpected slips during the sub-assembly test.

The test results showed that the size of the core plate (aspect ratio) was the most influential parameter on energy dissipation capacities among the design variables considered in this study. At the 14th loading step, the cumulative hysteretic energy of the specimens with a 60x16mm core plate (C60R100 and C60R150) turned out to be about two times larger than those of the specimens having a 42x16mm core plate (C42R100-1 and C42R100-2). In addition, the size of the channel sections (or P_{cr}/P_y) affected the capacity of the BRKB. The CPD of the specimen C60R150 was about 19% larger than that of the C60R100 at the 14th loading step. It was also observed that the size of the channel sections improved the ductility capacity by increasing the confinement effect.

The specimens developed in this study showed several patterns of failure mode: Strong axis buckling of the core plate occurred in the specimens C42R100-1 and C42R100-2. These specimens failed due to the detachment of the stiffener caused by the buckling of the core plate in the strong axis. The specimen C60R100 showed weak axis buckling of the core plate due to the loss of confinement. The specimen C60R150 fractured at the connection of the end of the core and gusset plates where the rubber sheet used as unbonded material was detached. The specimen C42R150-R with longer groove length unexpectedly fractured at the early loading step.

Acknowledgements

This work was supported by the National Research Foundation of Korea (NRF) grant funded by the Korea government (MEST) (2011-0010384 & 2011-0028552).

References

- Balendra, T., Sam, M.T., Liaw, C.Y. (1991) "Preliminary studies into the behaviour of knee braced frames subject to seismic loading." *Journal of Engineering structures*, 13(1), pp. 67-74.
- Suita, K., Inoue, K., Koetaka, Y., Ando, M., Byakuno, Y. (2006) "Full-scale test on weld-free building structure with knee brace dampers." *International conference on behaviour of steel structures in seismic areas*; Stessa 2006 pp. 533-540.
- Takeuchi, T., Hajjar, J.F., Matsui, R., Nishimoto, K., Aiken, ID. (2010) "Local buckling restraint condition for core plates in buckling restrained braces." *Journal of Constructional Steel Research*, 66(2), pp. 139-149.
- Yoshino, T., Karino, Y. (1971) "Experimental study on shear wall with braces: Part 2. Summaries of technical papers of annual meeting." *Architectural Institute of Japan, Structural Engineering Section*, pp. 403-404.
- Watanabe, A., Hitomoi, Y., Saeki, E., Wada, A., Fujimoto, M. (1988) "Properties of braced encased in buckling-restrained concrete and steel tube." *Proc. 9th World Conference on Earthquake Engineering*, Tokyo/Kyoto, Japan, pp. 719-724.
- Qiang, X. (2005) "State of the art of buckling-restrained braces in Asia." *Journal of Constructional Steel Research*; 61(6), pp. 719-724.
- Clark, P., Aiken, I., Kasai, K., Ko, E., Kimura, I. (1999) "Design procedures for buildings incorporation hysteretic damping devices." *Proceedings of the 69th Annual Convention, SEAOC, Sacramento, CA. (USA.)*, pp. 355-372.
- Choi, Y., Kim, J. (2009) "Evaluation of seismic energy demand and its application on design of buckling-restrained braced frames." *Structural Engineering and Mechanics*; 31(1), pp. 93-112.
- Black, C.J., Makris, N., Aiken, I.D. (2004) "Component testing, seismic evaluation and characterization of buckling-restrained braces." *Journal of the Structural Engineering*; 130(6), pp. 880-894.
- Tsai, K.C., Weng, C.H. (2002) "Experimental responses of double-tube unbonded brace elements and connections." Report No. CEER/R91-02, Center for Earthquake Engineering Research, National Taiwan

University.

- Fahnestock, L.A., Sause, R., Ricles, J.M.(2004) "Seismic response and performance of buckling-restrained braced frames." *Journal of the Structural Engineering*; 133(9) , pp. 1195-1204.
- Aristizabal-Ochoa, J.D.(1986) "Disposable knee bracing: improvement in seismic design of steel frames." *J. Struct. Engng ASCE*; 112(7), pp. 1544-1552.
- Sam, M., Balendra, T., Liaw, C. (1995) "Earthquake-resistant steel frames with energy dissipating knee elements." *Journal of Engineering Structures*; 17(5), pp. 334-343.
- Maheri, M.R. Kousari, R., Razazan, M.(2003) "Pushover tests on steel X-braced and knee-braced RC frames." *Journal of Engineering structures*; 25(13), pp. 1697-1705.
- Kim, J., Seo, Y.(2003) "Seismic design of steel structures with buckling-restrained knee braces." *Journal of Constructional Steel Research*; 59(2); 1477-1497
- Tremblay, R., Bolduc, P., Neville, R., DeVall, R.(2006) "Seismic testing and performance of buckling restrained bracing systems." *Canadian Journal of Civil Engineering*; 33(2), pp. 183-198.
- Mehmet, E., Cem, T.(2010) "An experimental study on steel-encased buckling-restrained brace hysteretic dampers." *Earthquake Engng Struct. Dyn.*; 39(5), pp. 561-581.
- AISC (2005). "Seismic provision for structural steel building" Chicago (IL): American Inst. of Steel Construction.
- SEAOC/AISC (2005). "Recommended provisions for buckling-restrained braced frame," Structural Engineers Association of California/American Institute of Steel Construction.
- Horie, T., Yabe, Y. (1993) "Elasto-plastic behavior of steel brace with restraint system for post buckling." *Annual Technical Papers of Steel Structures 1, Japan*, pp. 187-194.